Mon. Not. R. Astron. Soc. **000**, 1–14 (2010) Printed 17 March 2011 (MN LATEX style file v2.2)

Dynamics of the Magellanic Clouds in a ΛCDM Universe

Michael Boylan-Kolchin[1,2⋆], Gurtina Besla[3], and Lars Hernquist[3]
[1] *Max-Planck-Institut für Astrophysik, Karl-Schwarzschild-Str. 1, 85748 Garching, Germany*
[2] *Center for Galaxy Evolution, 4129 Reines Hall, University of California, Irvine, CA 92697, USA*
[3] *Harvard-Smithsonian Center for Astrophysics, 60 Garden Street, Cambridge, MA 02138, USA*

17 March 2011

ABSTRACT
We examine Milky Way-Magellanic Cloud systems selected from the Millennium-II Simulation in order to place the orbits of the Magellanic Clouds in a cosmological context. Our analysis shows that satellites massive enough to be LMC analogs are typically accreted at late times. Moreover, those that are accreted at early times and survive to the present have orbital properties that are discrepant with those observed for the LMC. The high velocity of the LMC, coupled with the dearth of unbound orbits seen in the simulation, argues that the mass of the MW's halo is unlikely to be less than $2 \times 10^{12}\,M_{\odot}$. This conclusion is further supported by statistics of halos hosting satellites with masses, velocities, and separations comparable to those of the LMC. We further show that: (1) LMC and SMC-mass objects are not particularly uncommon in MW-mass halos; (2) the apparently high angular momentum of the LMC is not cosmologically unusual; and (3) it is rare for a MW halo to host a LMC-SMC binary system at $z = 0$, but high speed binary pairs accreted at late times are possible. Based on these results, we conclude that the LMC was accreted within the past four Gyr and is currently making its first pericentric passage about the MW.

Key words: Galaxy: fundamental parameters – Galaxy: formation – galaxies: formation – galaxies: kinematics and dynamics – Magellanic Clouds

1 INTRODUCTION

The Milky Way and its satellite galaxies offer a unique laboratory for near-field cosmology. The proximity of Milky Way (MW) satellites means that their stellar content is resolved and can be used as a probe of galaxy formation and evolution (Grebel 2005). Furthermore, with the high astrometric precision of instruments such as the Advanced Camera for Surveys on the Hubble Space Telescope (HST), it is now also possible to measure accurate proper motions for some of these satellites (e.g., Kallivayalil et al. 2006a,b; Piatek et al. 2007, 2008). These measurements have significantly improved constraints on the satellites' orbital histories, and have also revealed some surprises. In particular, Kallivayalil et al. (2006a, hereafter K06) found that the velocity of the Large Magellanic Cloud (LMC) is approximately $380\,\mathrm{km\,s^{-1}}$, which is much larger than what typically had been assumed ($\lesssim 300\,\mathrm{km\,s^{-1}}$; e.g., Gardiner & Noguchi 1996) in modeling the orbit of the LMC.

This large velocity has forced a reconsideration of the conventional picture of the orbital history of the Magellanic Clouds (MCs), wherein the MCs have made multiple passages about the MW over a Hubble time. K06 and Besla et al. (2007, hereafter, B07) analyzed possible LMC orbits and divided them into two categories: early accretion, in which the LMC has made at least one complete orbit about the Milky Way; and late accretion, where the LMC is currently making its first pericentric passage. Distinguishing between these two orbital histories has important consequences for our understanding of the Local Group's assembly history and for the formation of the Magellanic Stream (Besla et al. 2010).

The high velocities of the Clouds also raise the question of whether the MCs' orbits are typical of massive satellites in MW-like systems and whether they can provide information about the mass of the MW's halo. B07 showed that the MCs are effectively on an unbound orbit if the MW's mass is on the low end of current estimates ($\sim 10^{12}\,M_{\odot}$, consistent with the results of Xue et al. 2008 based on blue horizontal-branch stars). On the other hand, a massive MW halo ($\sim [2-2.5]\times 10^{12} M_{\odot}$) – in line with estimates based on the timing argument and satellite kinematics including data from Leo I (Li & White 2008; Watkins et al. 2010) – implies that the LMC has a velocity that is substantially lower than the local escape speed.

Analyses of cosmological simulations indicate that unbound orbits are quite rare (van den Bosch et al. 1999; Vitvitska et al. 2002; Benson 2005; Khochfar & Burkert

⋆ e-mail: m.bk@uci.edu

2006; Diemand et al. 2007; Wetzel 2010): for example, Wetzel (2010) found that less than 2% of merging satellites have formally unbound orbits at all masses and redshifts. Sales et al. (2007) have shown that a non-negligible number of subhalos in cosmological simulations can be scattered to high energy orbits as the result of three-body encounters, but these subhalos are dynamically required to be low-mass, likely rendering this mechanism irrelevant for the LMC. Almost all of these results are based on modeling dark matter halos as point mass, Kepler potentials. This is a poor approximation to the true structure of dark matter halos at small radii, however. The LMC, which is currently at $\lesssim$ one-fifth the MW's virial radius, is in precisely this regime. As a result, it is far from clear whether an unbound LMC would be highly unusual in a cosmological context.

The very existence of massive satellites such as the MCs can also be used to place constraints on the mass of the MW. If the LMC is typical for galaxies of its stellar mass, it likely had a dark matter mass of $[1-2]\times10^{11}\,M_\odot$ before accretion by the MW (Guo et al. 2010; Boylan-Kolchin et al. 2010). The SMC has a stellar mass that is typical for halos that are only a factor of 2-3 less massive than this. Boylan-Kolchin et al. (2010, hereafter BK10) used statistics of subhalos from a large sample of simulated MW-mass halos to conclude that MC-mass galaxies are rare if the MW has $M \lesssim 10^{12}\,M_\odot$ but are much more typical if the MW has a massive dark matter halo ($\sim 2.5\times10^{12}$). These results were based purely on the masses of the MCs and MW, however, and did not include the additional constraints provided by the MCs' orbits.

In this paper, we examine the orbits, accretion epochs, and masses of MW-MC systems using the Millennium-II Simulation (MS-II; Boylan-Kolchin et al. 2009), which has sufficient mass resolution to probe SMC-mass scales and a large enough volume to contain a large, statistical sample of MW-mass halos. We use realistic – but still spherically-symmetric – potentials that are expected for LCDM dark matter halos when computing orbital parameters in an attempt to accurately describe the orbits of MC analogs at small radii from their hosts.

Our goal is to investigate five main questions related to the MCs in order to place their orbital properties and masses in a cosmological context:

- How common are satellites with masses similar to those of the LMC and SMC within Milky Way-mass halos at redshift zero?
- How typical is the LMC in terms of its orbital properties (e.g., energy and angular momentum)?
- Are LMC-type satellites at $z = 0$ typically accreted **early** (having completed at least one pericentric passage about their hosts) or **late** (being on their first infall towards their hosts)?
- How likely is it that the MCs were accreted as a binary system?
- What can we infer about host halos from the properties of massive satellites such as the LMC?

Our work is structured as follows. § 2 provides relevant details about the MS-II, describes our assumptions about the MW and MCs, and defines our subhalo samples. In § 3.1, we determine the most likely accretion epoch for the LMC based on mass considerations. In § 3.2-§ 3.4, we fold the orbital properties of the LMC into the analysis to distinguish between the early or late accretion scenarios. Section 4 explores the expected frequency of L/SMC-type companions about MW-type hosts based on the MCs' expected infall masses. In § 5, we examine potential L/SMC binary systems and their properties. Our results are discussed in § 6; in particular, we assess the likelihood that the MCs are on their first passage about the MW (§ 6.2). We present our conclusions in § 7.

2 METHODOLOGY

2.1 The Millennium-II Simulation

Our analysis of objects similar to the Magellanic Clouds is based on the Millennium-II Simulation, a very large N-body simulation that follows the evolution of over ten billion particles in a periodic cube of $(137\,\mathrm{Mpc})^3$ from redshift 127 to 0. The cosmological parameters used in the MS-II are identical to those adopted for the Millennium Simulation (Springel et al. 2005) and the Aquarius simulations (Springel et al. 2008):

$$\Omega_{\rm tot} = 1.0,\ \Omega_m = 0.25,\ \Omega_b = 0.045,\ \Omega_\Lambda = 0.75,$$
$$h = 0.73,\ \sigma_8 = 0.9,\ n_s = 1\,, \qquad (1)$$

where h is the Hubble constant at redshift zero in units of $100\,\mathrm{km\,s^{-1}\,Mpc^{-1}}$, σ_8 is the rms amplitude of linear mass fluctuations in $8\,h^{-1}\,\mathrm{Mpc}$ spheres at $z = 0$, and n_s is the spectral index of the primordial power spectrum. The MS-II offers a unique combination of mass resolution and large volume for studying dynamics of Magellanic Cloud analogs within Milky Way-mass systems: the MS-II particle mass of $m_p = 9.43\times10^6\,M_\odot$ results in over 100,000 particles in Milky Way-mass halos at $z = 0$, and resolves LMC-mass subhalos with $\gtrsim 10,000$ particles. For further information about the MS-II, see Boylan-Kolchin et al. (2009).[1]

2.2 Milky Way-mass halos

Current estimates of the mass of the Milky Way's halo range from $\approx [1-3]\times10^{12}\,M_\odot$ (e.g., Sakamoto et al. 2003; Battaglia et al. 2005; Dehnen et al. 2006; Xue et al. 2008; Li & White 2008; Gnedin et al. 2010; Watkins et al. 2010; and references therein). In order to bracket this range, and to understand any trends with the mass of the MW, we select all halos with $4.3\times10^{11} \le M_{\rm vir}/M_\odot \le 4.3\times10^{12}$ from the MS-II at redshift zero as our primary "Milky Way" sample. This set is identical to that of Boylan-Kolchin et al. (2010) and contains approximately 7600 dark matter halos, 2658 of which have $M_{\rm vir} \in [1-3]\times10^{12}\,M_\odot$. It is important to note that not all of these halos are expected to host MW-like galaxies in the standard ΛCDM model: for exmple, approximately 30% of halos in our full MW sample should host galaxies that are not late-type based on their colors and specific star formation rates (Weinmann et al. 2006). By taking subsets of our main sample that are based on,

[1] Merger trees, along with halo and subhalo catalogs, from the MS-II are publicly available at http://www.mpa-garching.mpg.de/galform/millennium-II/ .

e.g., environment, we can explore whether host halo properties correlate with the likelihood of hosting satellite galaxies like the MCs.

We use the radius inside of which the average density exceeds the critical density of the universe by a factor $\Delta_{\rm vir}$ (see Eke et al. 1996 and Bryan & Norman 1998 for details) as the virial radius $R_{\rm vir}$ of our halos, and the mass enclosed within this radius, $M_{\rm vir}$, as the virial mass. At redshift zero in the cosmology of the Millennium-II Simulation, $\Delta_{\rm vir} = 94.2$ and the virial radius $R_{\rm vir}$ and virial (circular) velocity $V_{\rm vir}$ scale with the virial mass as:

$$R_{\rm vir} = 257.8 \left(\frac{M_{\rm vir}}{10^{12}\,M_\odot}\right)^{1/3} {\rm kpc} \quad (2)$$

$$V_{\rm vir} = 129.2 \left(\frac{M_{\rm vir}}{10^{12}\,M_\odot}\right)^{1/3} {\rm km\,s^{-1}}\,. \quad (3)$$

We will use these relations in subsequent sections to scale measured properties of the Magellanic Clouds – e.g., their angular momenta – to the virial values for a range of virial masses for the MW.

Later sections will also focus on orbital properties of subhalos within their hosts. These properties will be computed assuming that the host dark matter halos are well-fitted by Navarro, Frenk, and White (1996, 1997; hereafter, NFW) density profiles. The structure of the NFW profile is fully specified by a halo's mass and the radius at which the circular velocity curve peaks, $R_{\rm max}$. Using values of $M_{\rm vir}$ and $R_{\rm max}$ computed directly from the MS-II to set the NFW potential, we calculate the energy, angular momentum, and eccentricity of orbiting subhalos within MW-mass hosts[2]. We defer an analysis of the current distance of the LMC from the MW to Section 6.3, as it is inherently extremely rare for a satellite to be near pericenter (as is the case for LMC) for the eccentric orbits typical of ΛCDM satellites (Tormen 1997; Diemand et al. 2007). Note that one limitation of our approach is the use of spherically symmetric profiles in our calculations, whereas halos from cosmological dark matter simulations are typically prolate or triaxial (e.g., Warren et al. 1992; Jing & Suto 2002; Allgood et al. 2006; Bett et al. 2007).

2.3 The Magellanic Clouds

2.3.1 Observed properties

The Large (Small) Magellanic Cloud is the most (second-most) luminous satellite of the Milky Way. Following Kim et al. (1998), we assume that the stellar mass of the LMC is $M_{\rm LMC,\star} = 2.5\times10^9\,M_\odot$. We adopt a galactocentric distance of $R_{\rm LMC} = 50.1\,{\rm kpc}$ (Freedman et al. 2001). K06's analysis of the LMC's proper motion shows that

$$\begin{aligned} V_{\rm LMC,tan} &= 367 \pm 18\ {\rm km\,s^{-1}} \\ V_{\rm LMC,rad} &= 89 \pm 4\ {\rm km\,s^{-1}}\,. \end{aligned} \quad (4)$$

[2] We assume a fixed concentration of 10 when computing the potential of the actual MW. This is not a strong assumption, as changing the concentration between, e.g., 8 & 12 does not significantly affect the inferred pericenter, angular momentum, or orbital energy of the subhalos.

The specific angular momentum of the LMC, normalized by the specific angular momentum of a circular orbit at the MW's virial radius, is therefore

$$\widetilde{j}_{\rm LMC} \equiv \frac{R_{\rm LMC}\,V_{\rm LMC,tan}}{R_{\rm vir}\,V_{\rm vir}} = 0.55\left(\frac{M_{\rm vir}}{10^{12}\,M_\odot}\right)^{-2/3}\,. \quad (5)$$

We assume that the SMC is at a distance of 58.9 kpc (Kallivayalil et al. 2006b) and has a stellar mass of $M_{\rm SMC,\star} = 3\times10^8\,M_\odot$ (Stanimirović et al. 2004). The proper motion measurements of Kallivayalil et al. (2006b) give

$$\begin{aligned} V_{\rm SMC,tan} &= 301 \pm 52\ {\rm km\,s^{-1}} \\ V_{\rm SMC,rad} &= 23 \pm 7\ {\rm km\,s^{-1}}\,. \end{aligned} \quad (6)$$

From these values, the specific angular momentum of the SMC is

$$\widetilde{j}_{\rm SMC} \equiv \frac{R_{\rm SMC}\,V_{\rm SMC,tan}}{R_{\rm vir}\,V_{\rm vir}} = 0.53\left(\frac{M_{\rm vir}}{10^{12}\,M_\odot}\right)^{-2/3}\,. \quad (7)$$

The angular momenta of the LMC and SMC are therefore strikingly close to each other.

Piatek et al. (2008) have performed an independent analysis of the HST proper motion data and find results that are in general agreement with, but at the lower end of, the range found by K06. In particular, Piatek et al. find $(V_{\rm tan}, V_{\rm rad})$ of $(346\pm8.5\,{\rm km\,s^{-1}}, 93.2\pm3.7\,{\rm km\,s^{-1}})$ and $(259\pm17\,{\rm km\,s^{-1}}, 6.8\pm2.4\,{\rm km\,s^{-1}})$ for the Large and Small MCs, respectively. Adopting these values changes the normalization of Eqn. (5) to 0.52 and of Eqn. (7) to 0.46. Recently, Vieira et al. (2010) determined proper motions for the MCs using photographic and CCD observations from the Yale/San Juan Southern Proper Motion program spanning a baseline of 40 years. They also confirm the K06 results and find proper motions for the SMC that are more consistent with the Kallivayalil et al. (2006b) analysis than that of Piatek et al.

2.3.2 Magellanic Clouds in the Millennium-II Simulation

In order to identify $z = 0$ analogs of the LMC, we first search our full MW sample for all subhalos that survive to $z = 0$ and reside within a fixed fraction of $R_{\rm vir}$ of their host (see below). For each of these subhalos, we also find the mass of its main progenitor at all earlier times. To define analogs of the Magellanic Clouds in an N-body simulation such as the MS-II, we need a way to link dark matter (sub)halos to galaxies. Recent work has shown that many observed statistical properties of galaxies can be reproduced under the simple "abundance matching" assumption that stellar mass is a monotonically increasing function of the maximum dark matter mass a subhalo attains over its history (e.g., Conroy et al. 2006; Wang et al. 2006; Moster et al. 2010; Guo et al. 2010; Klypin et al. 2010). Accordingly, we select as our fiducial sample the subhalo with the largest maximum main progenitor mass in each halo; we will refer to this sample as the first-ranked subhalos. The mass of this progenitor and the redshift at which it was reached are denoted $M_{\rm acc}$ and $z_{\rm acc}$; we will sometimes refer to these quantities as the infall mass and infall redshift. Note that subhalos selected in this manner are not necessarily the most massive subhalos in their hosts at $z = 0$.

We identify LMC analogs within this sample by adding

two additional conditions. First, the host halos must obey $M_{\rm vir} \in [1-3] \times 10^{12}\,M_\odot$, corresponding to approximately 35% of our full host halo sample; note that this is in the upper end of our host sample in terms of mass. Next, we use abundance matching as implemented by Guo et al. (2010) to estimate the maximum dark matter halo mass of the LMC. With our definition of halo mass, the infall halo mass corresponding to the LMC's stellar mass is $M_{\rm LMC}(z_{\rm acc}) \approx 1.6 \times 10^{11}\,M_\odot$. We define LMC analogs as first-ranked subhalos having infall masses within a factor of two of this mass, $8 < M_{\rm LMC}(z_{\rm acc})\,[10^{10}\,M_\odot] < 32$, which allows for both scatter in the $M_\star - M_{\rm halo}$ relation and uncertainty in the stellar mass of the LMC. Such subhalos are more massive than the typical most massive subhalo, in terms of maximum progenitor mass, of MW-mass halos (BK10; see §4 for a full analysis).

To identify SMC analogs, we first find the surviving subhalos at $z = 0$ having the second highest infall mass among all subhalos of their hosts; we will refer to this fiducial sample as the second-ranked subhalos. Using the SMC's stellar mass, we select second-ranked subhalos with masses between 4×10^{10} and $1.6 \times 10^{11}\,M_\odot$ in hosts with $M_{\rm vir} \in [1-3] \times 10^{12}\,M_\odot$ as our SMC analogs. All SMC analogs therefore have at least 4000 particles at their maximum, well above the ~ 1500 particle requirement that Guo et al. (2010) show is necessary to adequately resolve the $M_{\rm acc}$ halo + subhalo mass function at $z = 0$ (see also Wetzel & White 2010).

It is important to choose a suitable limiting radius for defining each halo's most (second-most) massive surviving subhalo. A natural choice is the redshift zero virial radius. We therefore consider the most (second-most) massive non-dominant subhalo within $R_{\rm vir}$ at $z = 0$ as our fiducial sample. The precise choice of limiting radius used is not particularly crucial, so long as the radius is sufficiently large to cover much of the halo: we find similar results for $0.65 - 1.0\,R_{\rm vir}$.

To summarize, we define two samples for both the LMC and the SMC:

- **first-ranked subhalos** (1st):
the most massive subhalo, in terms of the maximum mass ever attained, located within $R_{\rm vir}$ of a host's center at $z = 0$. This sample contains 7641 subhalos.

- **LMC analogs**:
the subset of **1st** with $8 \times 10^{10} < M_{\rm acc}/M_\odot < 3.2 \times 10^{11}$ located in hosts with virial mass $M_{\rm vir} \in [1-3] \times 10^{12}\,M_\odot$. This sample contains **938** subhalos.

- **second-ranked subhalos** (2nd):
the second most massive subhalo, in terms of the maximum mass ever attained, located within $R_{\rm vir}$ of a host's center at $z = 0$. This sample contains 7639 subhalos.

- **SMC analogs**:
the subset of **2nd** with $4 \times 10^{10} < M_{\rm acc}/M_\odot < 1.6 \times 10^{11}$ located in hosts with virial mass $M_{\rm vir} \in [1-3] \times 10^{12}\,M_\odot$. This sample contains **840** subhalos.

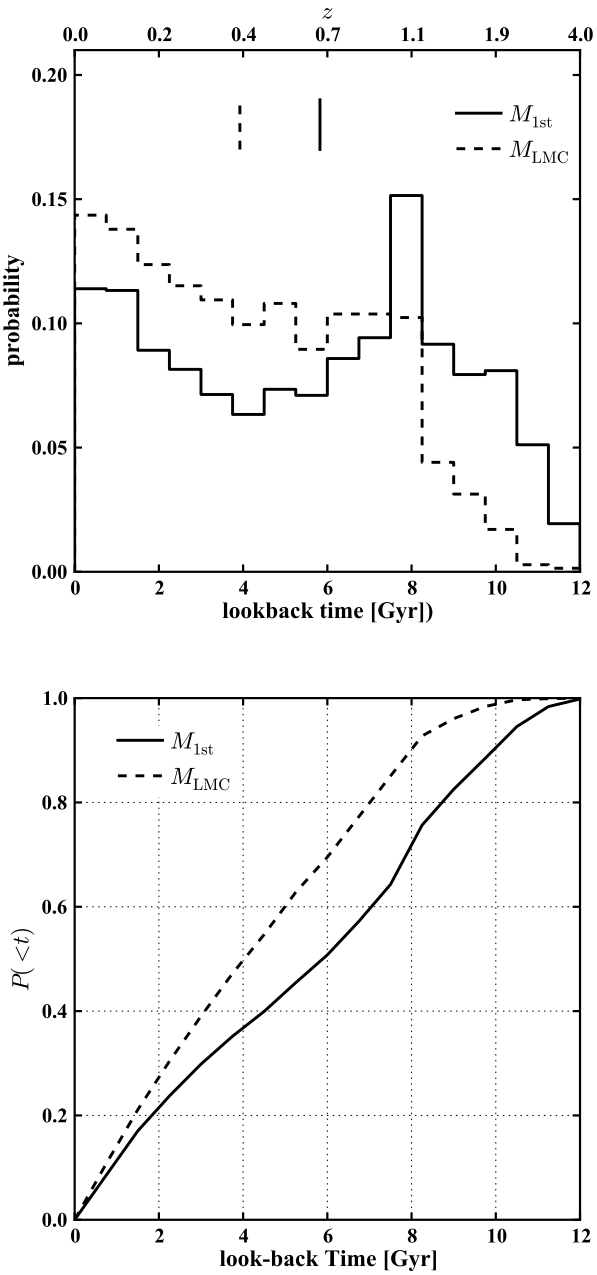

Figure 1. *Top:* Lookback time when the 1st ranked subhalo (solid histogram) or LMC analog (dashed histogram) first crossed the physical $z = 0$ virial radius of its host. Vertical lines mark the medians of the distributions. *Bottom:* Cumulative version of the upper plot. 50% of LMC analogs were accreted by MW-mass hosts within the past 4 Gyr and 25% within the past 2 Gyr.

3 ORBITAL PROPERTIES OF LMC CANDIDATES

3.1 First crossing time

The lookback time at which the LMC first crossed the physical $z = 0$ virial radius of the MW, moving inward – referred to hereafter as the first crossing time ($t_{\rm fc}$) – serves as a useful discriminant between the early and late accretion scenarios laid out in B07. We therefore compute $t_{\rm fc}$ for all first-ranked

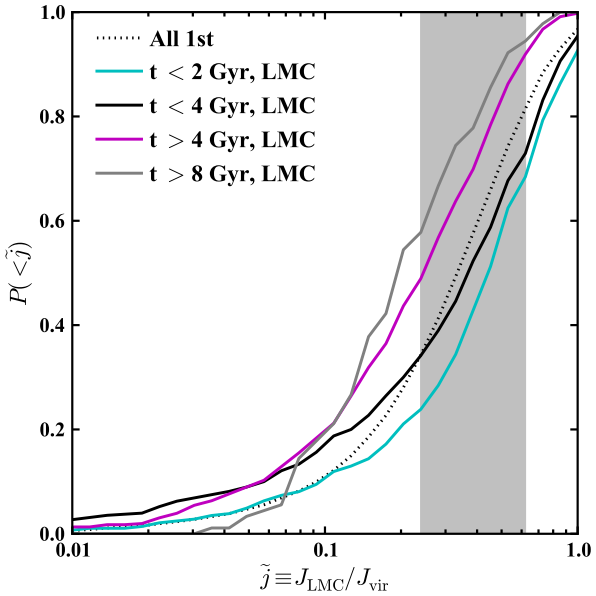

Figure 2. Distribution of (specific) angular momentum for LMC analogs accreted early (more than 4 Gyr ago; magenta) and late (within the last 4 Gyr; black), as well as very early (more than 8 Gyr ago; gray) and very late (less than 2 Gyr ago; cyan). Also plotted is the cumulative distribution for all 1st-ranked subhalos, independent of accretion epoch (black dotted line). The gray shaded region corresponds to the observed angular momentum of the LMC, including $\pm 2\sigma$ errors on the tangential velocity, for a Milky Way mass in the range $[1-3]\times 10^{12}\,M_\odot$. Late-accreted LMCs typically have higher specific angular momentum, due to both the inefficiency of dynamical friction over ~ 3 Gyr timescales and the higher specific angular momentum of late-accreted subhalos.

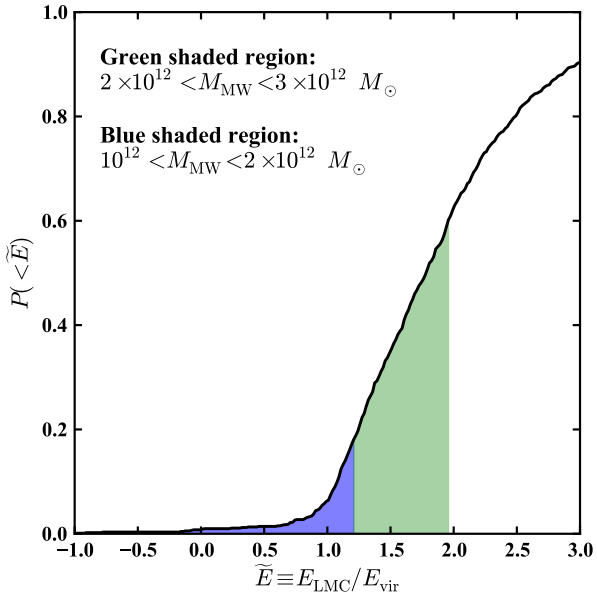

Figure 3. Distribution of orbital energies for the LMC analogs relative to the energy of a circular orbit at the host's virial radius. Blue and green shaded regions correspond to hosts of $[1-2]\times 10^{12}$ and $[2-3]\times 10^{12}\,M_\odot$, respectively. Unbound orbits ($\widetilde{E}<0$) are extremely rare, as are orbits consistent with a low-mass ($\lesssim 1.5\times 10^{12}\,M_\odot$) MW.

halos in our full MW sample to investigate whether there is a preferred accretion epoch for LMC-like objects.

The distributions of $t_{\rm fc}$ for all first-ranked subhalos and for those in the LMC analog subsample are shown in Fig. 1 as solid and dashed histograms, respectively. The full distribution is bimodal, with a primary peak at $t\approx 8$ Gyr and a secondary peak at $t=0$ Gyr; the median value is $t_{\rm fc}=5.8$ Gyr. The distribution for the LMC-mass sample is markedly different. There is no prominent peak at $t_{\rm fc}\approx 8$ Gyr; instead, the distribution rises continuously from large lookback times (high redshift) to the present day, and the median of the distribution lies at $t_{\rm fc}=3.9$ Gyr. The differences between the two distributions reflect the relatively high masses of the LMC analog sample: since these subhalos are more massive than the average first-ranked subhalo, they are accreted onto their host halos later, in the typical hierarchical manner expected in the ΛCDM cosmology.

Candidates in the LMC's expected mass range are usually accreted at fairly late times: only 12% have $t_{\rm fc}>7.5$ Gyr ($z_{\rm fc}>1$), while approximately 30% have been accreted within the past 2 Gyr. Such numbers favor the late accretion scenario for the LMC. Even taking all first-ranked subhalos (the solid line in the lower panel of Fig. 1), we find that $\sim$ 70% were accreted since $z=1$. First-ranked subhalos that could have completed several orbits are rare.

3.2 Angular momentum

Figure 2 shows the cumulative distribution of specific angular momenta[3] $j=RV_{\rm tan}$, normalized by the virial value $j_{\rm vir}=R_{\rm vir}V_{\rm vir}$, for the full 1st-ranked subhalo sample (dotted line). Also plotted is the same quantity for LMC analogs, split based on their accretion times: less than 2 and 4 Gyr ago (cyan and black lines, respectively), and more than 4 and 8 Gyr ago (magenta and gray lines). The gray shaded region marks the range of $\widetilde{j}=j/j_{\rm vir}$ allowed for the LMC based on a MW mass of $10^{12}\le M_{\rm vir}\le 3\times 10^{12}\,M_\odot$ and including $\pm 2\sigma$ on the LMC's tangential velocity. This allowed range is fairly broad and shows that the angular momentum of the observed LMC is, in fact, fairly typical of LMC analogs in the MS-II.

Comparing the angular momentum of LMC analogs based on accretion epoch, we find that LMCs accreted $>$ 4 Gyr ago have much lower angular momentum than those accreted at later times. In fact, 50% of those LMCs accreted $>$4 Gyr ago have angular momentum lower than the observed range for the LMC. On the other hand, half of the LMC analogs accreted within the past 2 Gyr have angular momentum within the shaded region, supporting a late accretion scenario for the LMC.

[3] The angular momentum is computed with respect to the host's center, defined by the location of the gravitational potential minimum. The host's velocity is determined by averaging over all particles in the host's main subhalo. We have also tried computing the velocity with respect to only the most bound particles in the host subhalo or only those particles within 10 or 25 kpc and found that the results presented here are unchanged.

Early accreted (> 4 Gyr ago) LMC analogs in low-mass MWs are strongly disfavored: even in the most extreme scenario of $M_{\rm vir} = 3 \times 10^{12}$ and $V_{\rm tan,LMC} = 331\,{\rm km\,s^{-1}}$ ($2\,\sigma$ lower than the central value of K06), we still find that over 50% of LMC analogs have a lower value of $\widetilde{j}$ than for the actual LMC. A more realisitc scenario – $M_{\rm vir} = 1.6 \times 10^{12}$ and $V_{\rm tan,LMC} = 367\,{\rm km\,s^{-1}}$ – results 90% of early-accreted LMCs having lower angular momentum than is observed at $z = 0$.

Regardless of accretion epoch, approximately 30-35% of LMC analogs fall in the gray shaded region: the LMC's angular momentum is not atypical in a cosmological context. This result dismisses previous assertions that tidal torques from M31 are needed to explain the orbital angular momentum of the LMC (e.g., Raychaudhury & Lynden-Bell 1989; Shuter 1992; Byrd et al. 1994). Originally, concerns about the LMC's angular momentum arose because the orbital plane of the MCs is polar to the disk plane of the MW, while the LMC has orbital angular momentum that is at least as much as that of the MW's thin disk (Fich & Tremaine 1991; Lin et al. 1995; Sawa & Fujimoto 2005). This is potentially difficult to explain in an early accretion scenario: torques from the MW's disk certainly could not explain the angular momentum of the LMC in this configuration, leading to the search for alternate potential perturbers. While our analysis does not extend to the likelihood of a polar orbital orientation, we do find that the angular momentum of the LMC's orbit is more typical in a recent accretion scenario. Over such short interaction timescales, torques from the host are largely irrelevant and our result should hold regardless of the orientation of the orbit.

3.3 Energy

Figure 3 shows the orbital energy distribution of the MS-II LMC analogs, normalized by the energy of a circular orbit at the host's virial radius. A striking feature of Fig. 3 is that nearly all subhalos are on bound orbits ($\widetilde{E} \equiv E/E_{\rm circ}(R_{\rm vir}) > 0$). The implications of the energies of subhalos' orbits for the LMC are highly sensitive to the virial mass of the MW: less than 10% of LMC analogs have orbits as energetic as that of the observed LMC if the MW's virial mass is smaller than $2 \times 10^{12}\,M_\odot$ (blue shaded region), while a substantial fraction have orbits that match the energy of the LMC's orbit if the MW's halo lies between $[2-3] \times 10^{12}\,M_\odot$ (green shaded region). Even if we take both radial and tangential velocities that are $1\,\sigma$ ($2\,\sigma$) lower than K06's mean values, we still find that only 2.3% (7.9%) of orbits are more energetic than observed for the LMC in a halo of $1.5 \times 10^{12}\,M_\odot$.

In Figure 4 we show the cumulative distribution of $\widetilde{E}$ for the LMC analog sample, split by accretion epoch (solid curves); the distribution for the full LMC analog sample (Fig. 3) is shown as the dotted curve. There is a marked difference when looking at early (>4 Gyr) versus late (< 4 Gyr) accreted LMCs. Early-accreted LMCs tend to be on much more bound orbits (higher values of $\widetilde{E}$), while late-accreted LMCs are less bound to their host halos (though virtually all are still bound, formally).

Using the mean velocities from K06, we find that a Milky Way of mass $(1, 2, 3) \times 10^{12}\,M_\odot$ corresponds to $\widetilde{E} = (-0.53, 1.21, 1.96)$. If the Milky Way's halo mass does not exceed $2 \times 10^{12}\,M_\odot$, the early accretion scenario is strongly disfavored: there are vanishingly few early-accreted LMCs in the MS-II having $\widetilde{E} < 1.2$. Fig. 4 also strongly disfavors *any* LMC accretion scenario for a $10^{12}\,M_\odot$ MW (which puts the LMC on an unbound orbit). Approximately 25% of the late-accreted (and 7% of the early-accreted) LMCs have binding energies lower than the observed LMC for a MW mass of $2 \times 10^{12}\,M_\odot$. The energetics favor a combination of a massive MW halo and a late-accreted LMC.

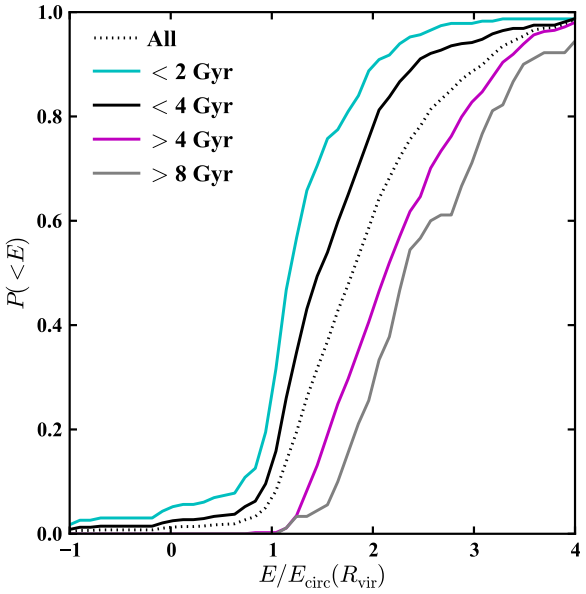

Figure 4. Orbital energies for the LMC analog sample (dotted curve), as well as results split by $t_{\rm fc}$ (solid curves). The early-accreted LMCs (> 4 Gyr, shown in magenta) are typically more bound to their host than are the late-accreted LMCs (< 4 Gyr, shown in black). This trend is even stronger for LMCs accreted over 8 Gyr ago (gray) versus those accreted within the past 2 Gyr (cyan).

3.4 Eccentricity

To further explore the typical orbital properties of surviving LMC analogs as a function of accretion epoch, we consider the distribution of orbital eccentricities for these systems. Orbital eccentricity e is here defined as a combination of the pericenters r_p and apocenters r_a of orbits:

$$e \equiv \frac{r_a - r_p}{r_a + r_p}\,. \tag{8}$$

(We assign unbound orbits an eccentricity larger than 1.) With this definition, $e < 0.5$ corresponds to fairly circular orbits ($r_a/r_p < 3$), while $e = 0$ indicates a perfectly circular orbit.

Figure 5 shows that early-accreted LMC analogs tend to be on orbits that are substantially more circular than those of late-accreted LMC analogs. Only 20% of LMCs accreted within the last 2 or 4 Gyr (cyan and black solid lines, respectively) have $e < 0.5$, a value that is met by approximately 50% of LMCs accreted over 4 Gyr ago and by 60% accreted

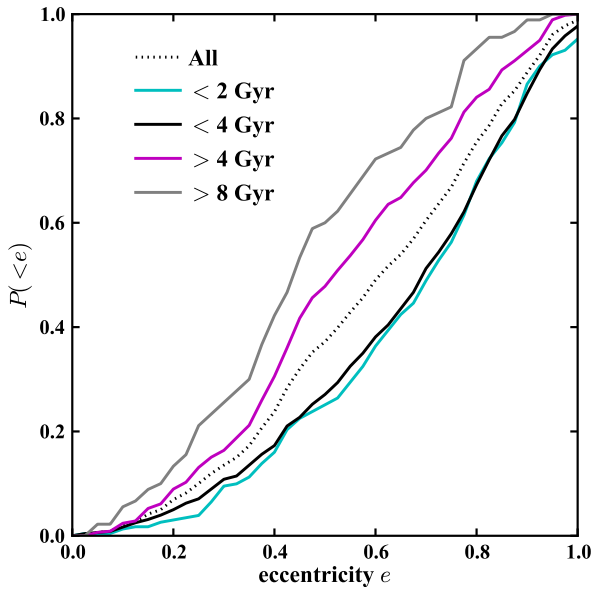

Figure 5. Orbital eccentricity for all LMC analogs (dotted line), as well as split by accretion epoch (solid lines). Early-accreted LMCs (gray and magenta lines) have orbits that are significantly more circular than do late-accreted LMCs (cyan and black). A MW of mass $(1.5, 2, 3) \times 10^{12}\,M_\odot$ corresponds to an LMC eccentricity of $(0.92, 0.79, 0.62)$, while a $10^{12}\,M_\odot$ MW results in an unbound orbit ($e > 1$).

more than 8 Gyr in the past. Although late accretion does not *a priori* mean that the Clouds cannot have completed multiple pericentric passages, these data on eccentricities provide further constraints. The mean eccentricity for the late-accreted LMC analogs is ~ 0.7. Given that the pericenter of the LMC's orbit is ~ 45 kpc, the resulting apocenter is ~ 260 kpc. The MCs clearly could not have completed multiple pericentric passages on such an orbit within the past 4 Gyr. We therefore conclude that the MCs were most likely accreted within the past 4 Gyr and are on their first passage about the MW

Fig. 5 reinforces how unlikely it is to find an object with the LMC's infall mass and orbit in a $10^{12}\,M_\odot$ halo at $z = 0$, regardless of accretion epoch, as the LMC has $e > 1$ according to our definition – i.e., the LMC's orbit is unbound – for this mass. If the MW *does* have such a low-mass halo, then the LMC was certainly accreted within the past 4 Gyr. Moreover, less than 10% of orbits – independent of accretion epoch – have $e > 0.92$, which corresponds to a halo mass of $< 1.5 \times 10^{12}\,M_\odot$. It is therefore quite unlikely that the Milky Way has a mass of less than $1.5 \times 10^{12}\,M_\odot$. (For reference, a Milky Way halo of mass $2 \times 10^{12}\,M_\odot$ results in an eccentricity of 0.79 for the LMC, while a mass of $3 \times 10^{12}\,M_\odot$ gives an eccentricity of 0.62.)

4 FREQUENCY OF LMC/SMC ANALOGS ABOUT MW HOSTS

In this section, we examine the mass distribution of the samples defined in § 2.3.2. Our goal is to determine how typical the infall masses of the MCs are relative to the full first- and second-ranked subhalo samples and as a function of the host mass.

The upper left panel of Fig. 6 shows the distribution of masses for first-ranked subhalos (solid histogram) and LMC analogs (dashed histogram), relative to the redshift zero virial mass of their hosts. The distribution of masses for first-ranked subhalos is fairly broad and peaks at $M_{\rm 1st} \approx 0.03 M_{\rm vir}(z = 0)$. The mass distribution of LMC analogs is substantially narrower and peaks at a much higher mass, $M_{\rm LMC} \approx 0.1 M_{\rm vir}(z = 0)$. The difference between the two distributions indicates that the LMC is more massive than the typical first-ranked satellite galaxy in a Milky Way-mass halo, a conclusion also reached in BK10.

A similar situation exists for the SMC, which is shown in the upper right panel of Fig. 6. While the distribution of $\mu_{\rm 2nd}$ peaks at ~ 0.01, the distribution of $\mu_{\rm SMC}$ peaks at ~ 0.03. This shows that the SMC is also more massive than the second-ranked galaxy in a typical MW-mass halo.

The solid line in the lower left panel of Fig. 6 shows the cumulative version of $M_{\rm 1st}(z_{\rm acc})/M_{\rm vir}(z = 0)$. The combined shaded region encompasses the full LMC analog sample; the range of $M_{\rm acc}/M_{\rm vir}(z = 0)$ corresponding to $M_{\rm vir} = 10^{12}\,M_\odot$ is shown in blue, while the range for $3 \times 10^{12}\,M_\odot$ in shown in gray. The lower right panel of Fig. 6 plots the same quantities for our sample of second-ranked subhalos and SMC analogs.

Recall that there are 2658 host halos in the mass range $M_{\rm vir} \in [1 - 3] \times 10^{12}\,M_\odot$. If we define MC analogs strictly in terms of mass, we thus conclude that approximately 35% of MW-mass halos host an LMC analog and 32% host an SMC analog within $R_{\rm vir}$. These numbers are for a specific range of MW halo masses, however, and are sensitive to the precise mass of the MW (BK10). A halo of $10^{12}\,M_\odot$ has a $\approx 20\%$ chance of hosting an LMC analog, and less than a 10% chance to host an SMC analog. A $3 \times 10^{12}\,M_\odot$ MW makes L/SMC analogs much more common, as approximately 40% of such hosts have L/SMC analogs. [Note that these numbers are likely to be upper estimates, as we have used very conservative estimates on the errors for the mapping between $M_\star$ and $M_{\rm acc}$.]

In a search for LMC analogs in the seventh data release of the Sloan Digital Sky Survey (York et al. 2000; Abazajian et al. 2009), Tollerud et al. (in prep.) determine that approximately 40% of isolated hosts with luminosities similar to that of the MW also have an LMC analog (r-band magnitude between -17.5 and -20) located within a projected separation of 250 kpc. Although the selection criteria of Tollerud et al. differ from those used here, this result appears consistent with our findings.

The mass of the first-ranked subhalo correlates strongly with its first crossing redshift $z_{\rm fc}$, which is shown in Fig. 7. The median (middle curve) decreases from $z_{\rm fc} \approx 1.4$ at $\mu = 0.01$ to 0.4 at $\mu = 0.1$ (70% of the distribution is contained within the dashed curves). The shaded region in Fig. 7 shows the allowed range for the LMC when using the abundance matching assumption (see Fig. 6)

An alternate way of looking at the dependence of μ(1st) on $z_{\rm fc}$ is to divide the 1st ranked subhalos into two samples: those accreted early, defined here as $z_{\rm fc} > 0.4$ (or equivalently, a look-back time of $t > 4$ Gyr, corresponding to the local minimum in Fig. 1), and those accreted at late times ($z_{\rm fc} < 0.4$ or $t < 4$ Gyr). The result of this split is shown in

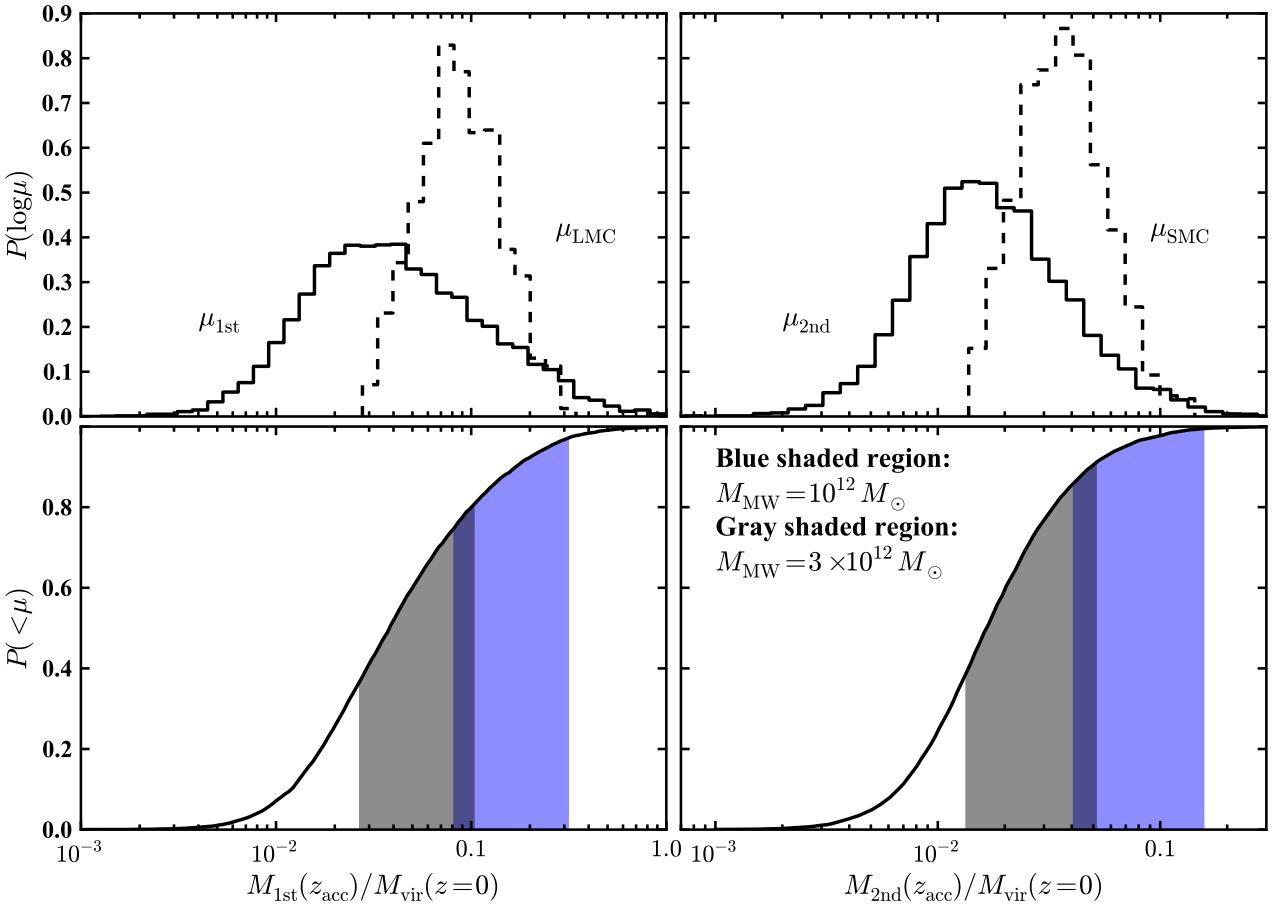

Figure 6. The distribution of masses of first-ranked subhalos (left panels) and second-ranked subhalos (right panels) with respect to the virial mass of their hosts. *Upper panels:* Distribution of $M_{\rm 1st}/M_{\rm vir}(z=0)$ and $M_{\rm LMC}/M_{\rm vir}(z=0)$ (solid and dashed histograms, left panel), and of $M_{\rm 2nd}/M_{\rm vir}(z=0)$ and $M_{\rm SMC}/M_{\rm vir}(z=0)$ (solid and dashed histograms, right panel). *Lower panels:* Cumulative distributions of solid curves from upper panels. The shaded regions correspond to the observed range of infall masses for the LMC (left panel) and SMC (right panel) assuming a MW mass of either $10^{12}\,M_\odot$ (blue region) or $3\times10^{12}\,M_\odot$ (gray region).

Fig. 8 and reinforces the result of Fig. 7: 1st ranked subhalos that have joined their $z=0$ host halos within the last 4 Gyr tend to be a factor of ~ 3 more massive at infall than those that joined their host halo more than 4 Gyr ago. Since the LMC has been shown to be more massive than the typical 1st ranked halo (see § 4), it is more likely to have been accreted at late times.

In order to assess whether a late or early accretion scenario is more plausible for the LMC, we need to also account for the survivability/mass loss expected for LMC analogs, which will depend on the accretion epoch and the specific orbit of the subhalo. Figure 9 shows the distribution of accretion mass relative to redshift zero dark matter mass[4] for LMC analogs. Results are plotted for early (more than 4 Gyr ago; cyan) and late (less than 4 Gyr ago; black) accretion epochs, as well as for very early (more than 8 Gyr ago; gray) and very recent (less than 2 Gyr ago; cyan) accretion epochs. There is a pronounced, and not unexpected, trend for stronger mass loss in earlier-accreted LMC analogs. The most recently accreted LMCs are typically a factor of 1.5-4 less massive at $z=0$ than at accretion (60% confidence interval), whereas the earliest accreted LMCs tend to be 3.5 to 30 times less massive. It is unlikely that the LMC could have undergone strong tidal stripping without losing much of its gas, which is at odds with observations.

Massive satellites typically do not survive for long before merging with their hosts: the dynamical friction timescale for a 1:10 object at $z=1$ is approximately 5 Gyr (Boylan-Kolchin et al. 2008), shorter than the time between $z=1$ and the present day. This is corroborated by Stewart et al. (2008), who showed that LMC-mass objects ($M\sim10^{11}\,M_\odot h^{-1}$) typically do not survive for more than $\sim$3 Gyr after accretion (their figure 5). BK10 examined the accretion epochs of massive subhalos in MW-mass hosts and found the same trend (their Fig. 12). Both groups argued, as we do here, that this lends support to a first passage scenario for the LMC.

[4] This is the bound mass determined by the `SUBFIND` algorithm.

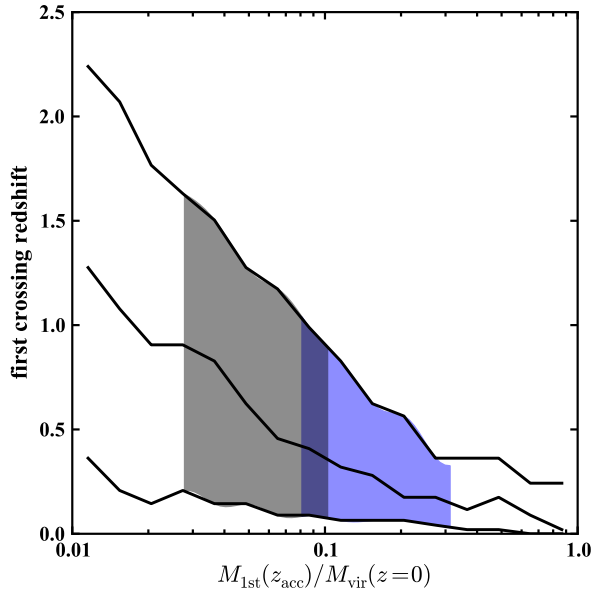

Figure 7. Redshift z_{fc} where the first-ranked subhalo first crossed the $z = 0$ virial radius of its host as a function of $M_{1st}/M_{vir}(z = 0)$. The middle line shows the median, while 70% of the distribution is contained between the upper and lower lines. The shaded region(s) are the same as in Fig. 6.

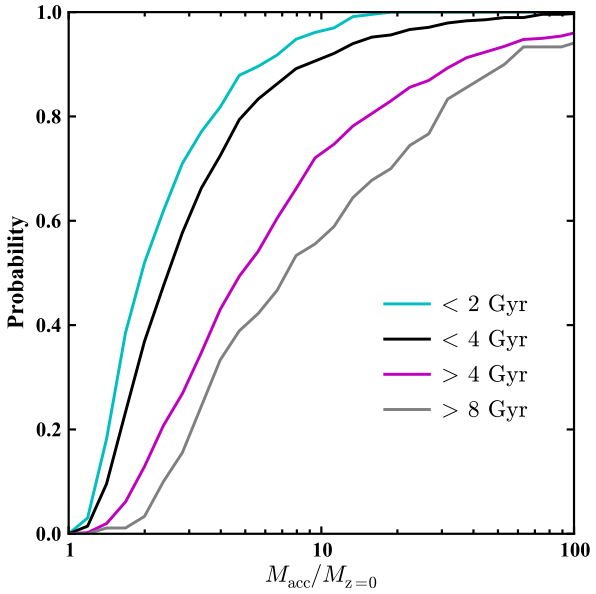

Figure 9. The cumulative distributions of infall mass relative to $z = 0$ mass (in dark matter) for LMC analogs. Each curve corresponds to LMC analogs with different accretion epochs. The most recently accreted candidates (cyan line) have typically lost of order half of their M_{acc}, whereas the earliest accreted LMCs (gray line) have lost almost 90% of their dark matter mass.

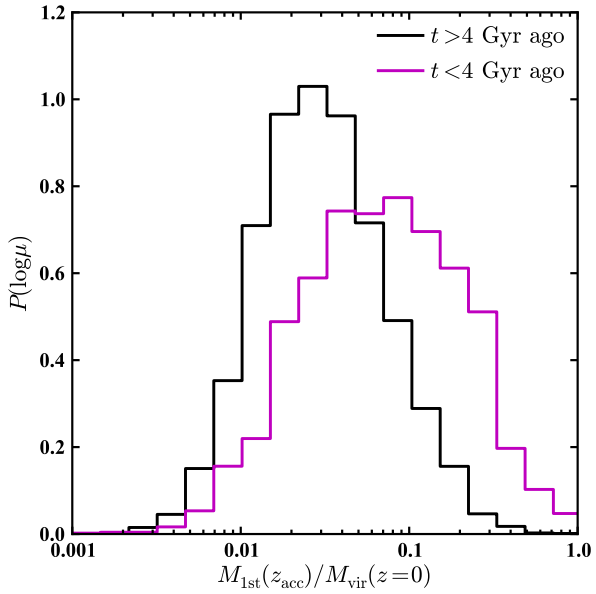

Figure 8. Distribution of masses for 1st ranked subhalos accreted early (more than 4 Gyr ago; black) and late (within the last 4 Gyr; magenta). Note that each distribution is separately normalized to unity; the number of first-ranked satellites with early accretion times is approximately 2.4 times greater than those with late accretion times. Those accreted at late times tend to be a factor of ∼3 more massive at infall than those accreted at early times.

5 LMC-SMC PAIRS

The small separation in position (∼20 kpc) and velocity space (∼100 km/s) between the two Magellanic Clouds makes it unlikely for them to be coincidental neighbors. Furthermore, the existence of (1) a bridge of gas connecting the two galaxies and (2) the Magellanic Stream, a stream of HI gas that trails behind the MCs over 150° across the sky, also strongly suggests that they have interacted for at least some time in the past (Besla et al. 2010).

These observations lead to a number of questions regarding the MC system, including: What is the probability that the MCs were accreted together and survive as a binary today? Is there a preferred accretion epoch or mass ratio for such a pair? How likely is it that the Clouds are only an apparent binary system today rather than a true binary system?

To this end, we consider the difference in accretion epoch between each LMC analog and the corresponding second-ranked halo about the same host. Figure 10 shows the median difference (solid line) in t_{fc} for the LMC analogs and second-ranked subhalos as a function of t_{fc} for the LMC analog, as well as the 10% (dotted) and 25% (dashed) quantiles. It is indeed possible to find first and second-ranked subhalos that are accreted as pairs (within 1 Gyr of each other). This probability depends on the LMC accretion epoch, however, and does not provide information about whether the accreted pairs can remain as a binary to the present day. The number of pairs accreted > 4 Gyr is approximately three times larger than the number accreted within the last 4 Gyr. This is likely a result of 1 Gyr being a much larger

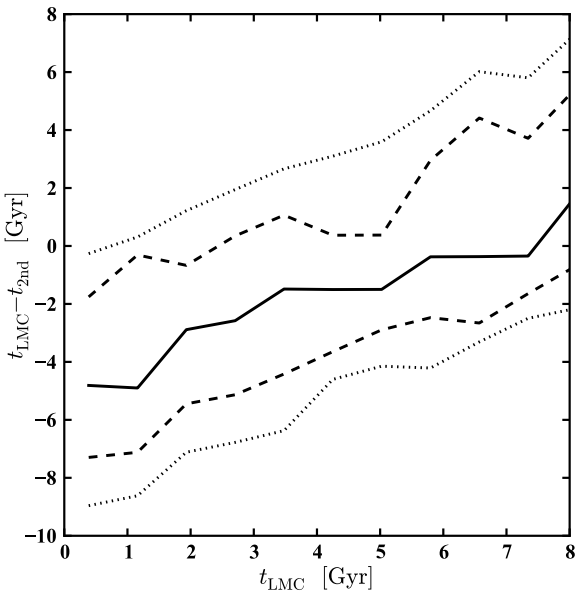

Figure 10. Difference in first crossing times between LMC analogs and the second ranked subhalo in each system as a function of the first crossing time of the LMC. (All times are lookback times.) The dotted (dashed) lines show the 10-90 (25-75) percentiles of the distribution, while the solid line shows the median. For LMCs with $t_{\rm fc} \sim 4$ Gyr, almost 40% of SMCs were accreted within ± 2 Gyr of the LMC, and 25% within ± 1 Gyr.

Table 1. Properties of LMC-SMC binaries. Column 1: ratio of masses of most massive progenitors; column 2: mass ratio at $z = 0$; column 3: first crossing time for LMC; column 4: first crossing time for SMC; column 5: separation between LMC and center of host; column 6: 3-D velocity of the LMC, relative to host.

$M_{\rm L}/M_{\rm S}$ $[z_{\rm acc}]$	$M_{\rm L}/M_{\rm S}$ $[z=0]^a$	$t_{\rm fc,LMC}$ [Gyr]	$t_{\rm fc,SMC}$ [Gyr]	$R_{\rm LMC}$ [kpc]	$V_{\rm LMC}$ [km/s]
11.74	20.01	0.00	0.26	244.39	121.92
2.79	24.29	0.26	0.00	323.87	221.25
6.42	16.27	0.54	0.26	180.25	225.66
6.69	32.02	0.83	1.13	151.70	287.50
3.20	1.30	1.44	1.13	26.09	417.31
15.07	15.52	1.44	1.44	82.97	57.49
7.76	16.18	1.76	1.13	98.58	127.10
12.61	33.32	2.77	2.43	172.74	41.07
1.11	2.60	2.77	7.56	88.77	124.46
1.15	1.83	3.13	3.49	124.35	153.10
1.35	2.25	3.49	5.73	41.78	99.13
7.19	15.53	4.23	4.97	115.93	121.54
21.24	151.66	4.97	4.60	148.06	129.51
1.39	21.76	5.35	7.91	95.29	132.18
2.57	3.43	5.73	4.97	232.48	175.78
1.86	13.26	6.47	5.73	104.46	163.18
3.41	12.83	6.47	10.06	39.37	240.08
5.27	9.49	6.84	7.20	107.45	92.04
1.40	7.25	7.20	9.20	141.99	82.45
1.77	0.83	7.20	10.06	57.44	22.06
11.47	25.43	7.56	10.06	72.74	127.48
1.45	0.73	7.56	9.20	94.08	25.78
3.83	3.32	8.58	7.91	107.39	229.95

[a] *Note that the calculation of subhalo masses at redshift zero is sensitive to the location of the subhalos within their hosts.*

fraction of a typical orbital time at higher redshifts than today.

We can also compute how likely it is to find MC-like objects around MW-mass hosts in a binary system at $z = 0$. To do so, we calculate the separation in position and velocity space between the LMC analog sample and the corresponding second-ranked subhalo for the same host. Systems having $|\Delta v| < 150\,{\rm km/s}$ and $|\Delta R| < 50\,{\rm kpc/h}$ are considered plausible binaries. Table 1 lists a number of properties for the 23 identified LMC/SMC analogs, including the first crossing time for each Cloud. Recall that the LMC analog sample contains 938 halos; it is thus possible, though not probable ($\sim 2.5\%$), that an LMC analog and a second ranked halo be found in a binary system about a MW-mass host today.

Since SMC analogs represent a subset of the second ranked subhalo sample, these numbers also indicate that LMC / SMC analogs accreted at similar epochs are not likely to exist as binaries at the present day. The binaries that do survive to $z = 0$ tend to have the SMC in an eccentric orbit about the LMC. This is in agreement with the proper motion measurements of the SMC by Kallivayalil et al. (2006b) and Vieira et al. (2010), who find a high relative velocity between the Clouds. An eccentric SMC orbit about the LMC is also required in the Magellanic Stream model proposed by Besla et al. (2010). The present study shows that such an orbital configuration is cosmologically expected.

A few specific cases from Table 1 stand out in particular. The first three rows have the pairs that were accreted most recently. All three of these systems have more angular momentum than the true LMC, highlighting that there may be no issue with the large magnitude of the LMC's angular momentum if it was accreted recently. Additionally, all are on fairly energetic orbits: with $E/E_{\rm vir} \approx 1$, these are the most energetic among all 23 binary candidates. In fact, most of the other candidates have $E/E_{\rm vir} \gtrsim 2$, which places them on orbits that are improbably bound (relative to the observed LMC) even for a MW of 10^{12}, $M_\odot$ (see Fig. 3). With the exception of the oldest binary candidate (the final row of Table 1), all systems with $t_{\rm fc}({\rm LMC}) > 5$ Gyr have low angular momentum, likely due to losses via dynamical friction. Although the volume of the MS-II does not provide a vast sample of possible binaries, those that do exist with orbital energetics similar to that observed for the Clouds are accreted at late times. Specifically, the systems highlighted in the first three rows of Table 1 illustrate that it is possible for a binary LMC/SMC to be accreted very recently on a high angular momentum/energy orbit

A further point of interest is that the pairs with first crossing redshifts that differ by $\gtrsim 2.5$ Gyr between the LMC and the corresponding second ranked subhalo are all cases where the LMC is within 100 kpc of the host. If these systems were true binaries, then there should also exist examples where the two subhalos had discrepant accretion epochs and are located at large distances from the host today. Since no such examples exist, it is likely that these are chance associations of two satellites near pericenter than true binaries.

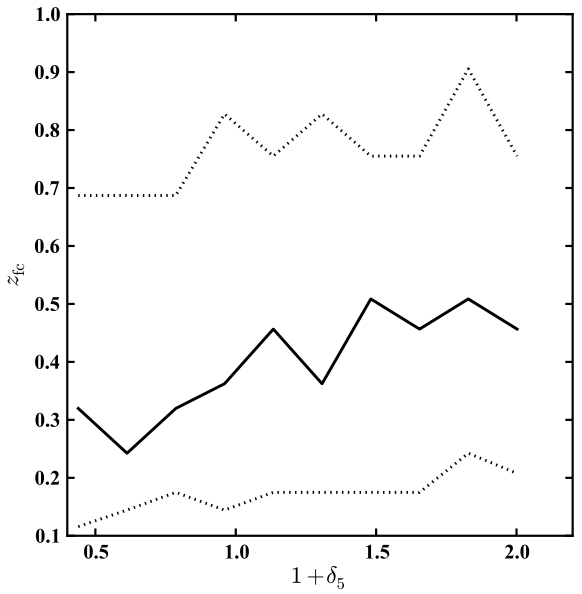

Figure 11. Dependence of $z_{\rm fc}$ on the large-scale overdensity, measured via gaussian smoothing on $5\,h^{-1}$ Mpc spheres, for the LMC analogs. There is no obvious dependence of $z_{\rm fc}$ on the large-scale overdensity, indicating that the large-scale environments of MW-mass hosts does not strongly influence the accretion epochs of their most massive subhalos.

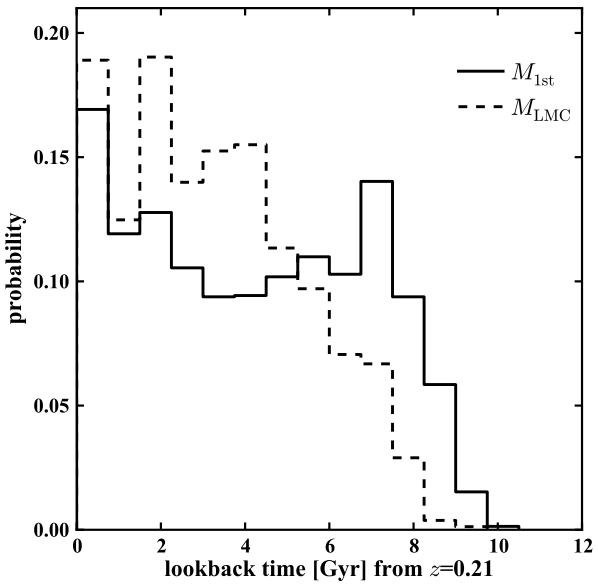

Figure 12. Distribution of first crossing times for the sample of MW-mass hosts selected at $z = 0.21$ (analogous to upper panel of Fig. 1). This distribution is similar to the distribution for $z = 0$ hosts, suggesting that changing σ_8 from 0.9 to 0.815 should not affect our conclusions on the probability of the LMC being on its first pass about the Milky Way.

6 DISCUSSION

Using the Millennium-II Simulation, we have investigated ΛCDM predictions for orbital properties and accretion histories of the MCs in the context of the updated proper motion measurements of Kallivayalil et al. (2006a,b). In this section, we further explore how environment or cosmological parameters may influence our results, the likelihood that the MCs are on their first passage about the MW, and the masses of halos hosting subhalos with LMC-like separations and velocities.

6.1 Milky Way sample

It is important to investigate whether the trends shown in the previous sections have any systematic dependence on any properties of the host halos. In particular, halos residing in low density environments have different accretion histories than those in high density regions (Gottlöber et al. 2001; Maulbetsch et al. 2007; Fakhouri & Ma 2010), an effect that could potentially bias our results on accretion epochs of LMC analogs. We therefore plot how the large-scale environment of a halo influences the first crossing redshift of LMC analogs in Fig. 11. This plot shows that $z_{\rm fc}$ is essentially independent of environment as measured by the dark matter overdensity, smoothed with a Gaussian filter of width $5\,h^{-1}$ Mpc. Our results should therefore be insensitive to the environment of the host halo.

The typical accretion epoch of LMCs could also be affected by the choice of cosmology in the MS-II, which has σ_8 that is approximately 10% higher than the current best-fitting value of ≈ 0.81 (Komatsu et al. 2009). [This difference is minor in terms of the number of MW-mass halos found at $z = 0$, as it affects the abundances of such halos by 10%.] While a quantitative understanding of the effects of varying σ_8 would require running a completely new simulation, we can easily estimate the qualitative effect by noting that lowering σ_8 results in later formation of halos of a given mass. We therefore expect that any changes due to reducing σ_8 would tend towards even later accretion epochs for LMC (and SMC) analogs.

Alternatively, we can note that $\sigma_8(z = 0.21) \approx 0.81$ for the MS-II cosmology; the difference between the distribution of $t_{\rm fc}$ for halos defined at this epoch and at $z = 0$ should therefore inform us about potential differences due to changes in the power spectrum normalization. The distribution of first crossing times for 1st-ranked subhalos and LMC analogs of halos selected from the MS-II at $z = 0.21$ (using the same criteria described in § 2) is shown in Fig. 12. Comparing this distribution with the distribution of $t_{\rm fc}$ in halos selected at $z = 0$ (the upper panel of Fig. 1), we can see that little changes between $z = 0$ and $z = 0.21$. Accordingly, reducing σ_8 from the Millennium and MS-II value of 0.9 is not likely to strongly affect our findings on the accretion epochs of LMC-like satellites.

6.2 Are the Magellanic Clouds on their first passage about the Milky Way?

A number of lines of observational evidence support the idea that the Magellanic Clouds are making their first pericentric pass about the Milky Way. This scenario explains why two gas-rich satellites reside at small galactocentric distances – similar satellites are typically found at much larger distances

from the MW or M31 (van den Bergh 2006) – as the Clouds would not have had sufficient interaction with the MW to have lost their gas by some combination of tidal stripping, harassment, and ram pressure stripping (Mayer et al. 2006). Similarly, the unusually blue color of the LMC (James & Ivory 2010; Tollerud et al., in preparation) means that it must have retained a substantial amount of star-forming gas, which is difficult to understand if the MCs have completed multiple orbits about the MW. The existence of stellar populations extending as far as ≈ 20 kpc from the LMC's dynamical center (Muñoz et al. 2006; Majewski et al. 2009; Saha et al. 2010) is also an indication that the LMC has not interacted strongly with the MW. Finally, Besla et al. (2010) have shown that the Magellanic Stream may originate from a tidal interaction between the MCs themselves, a model that requires the MCs to be a recently-accreted binary system.

B07 first examined the possibility that the MCs have been recently accreted by the MW using an orbital analysis constrained by the new HST proper motion measurements. Uncertainties in modeling the MW meant that a scenario in which the Clouds were accreted at early times cannot be ruled out by such an analysis (e.g., Gardiner & Noguchi 1996; Besla et al. 2007; Shattow & Loeb 2009), and refinements in the error space of the proper motions are unlikely to improve this situation. (We note, however, that early accretion models assume a static MW halo potential over a Hubble time, which is unrealistic.) We have computed the likelihood of a first passage scenario using a large sample of MW-mass halos from a high resolution cosmological simulation of the ΛCDM cosmology. Our results put the first passage scenario on even firmer ground. We have showed that it is highly improbable for surviving satellites with infall masses similar to that of the LMC to have been accreted at $z > 1$, rendering an early infall scenario unlikely based on mass considerations alone. We further found that 25% of surviving LMC analogs have been accreted within the past 2 Gyr and that the energetics of the LMC orbit are strongly inconsistent with the properties of LMC analogs accreted > 4 Gyr ago. Finally, we have showed that recently-accreted LMCs are incapable of making multiple pericentric passages by the present. Taken together, these results demonstrate that it is quite likely that the MCs have recently joined the MW and are currently making their first pericentric pass; a *very* recent accretion ($\lesssim$ 2 Gyr ago) is also cosmologically plausible.

6.3 Mass of the Milky Way

Uncertainties in the mass of the Milky Way's halo play a substantial role in placing the LMC and its orbit in a cosmological context, as has been shown repeatedly in our analysis. A low mass halo ($M_{\rm vir} \approx 10^{12}\,M_\odot$) means that the LMC is fairly unusual in terms of its (high) mass and that it is *very* unusual in terms of its (energetic) orbit. Both the mass and orbital energy of the LMC are more typical for halos of $M_{\rm vir} \gtrsim 2\times10^{12}\,M_\odot$.

We can also take an "inverse" view and ask, in what mass dark matter halo do objects with masses, velocities, and halo-centric distances similar to the LMC reside? To this end, we build a sample of LMC analogs with no constraint on the properties of the host halo (note that this differs from the mass-selected samples used up to this point). We merely require the following properties of the subhalo: (1) $0.8 < M_{\rm acc}\ [10^{11}\,M_\odot] < 3.2$, (2) $35 < R < 65\,$kpc from its host, and (3) $300 < V_{\rm tot} < 420\,{\rm km\,s^{-1}}$. Since these criteria are somewhat restrictive, we search for hosts in all 10 MS-II snapshots with $z < 0.3$. We find 495 subhalos matching our search criteria; the distribution of host halo masses for these matches are shown in Fig. 13. The figure confirms that satellites with properties similar to those of the LMC are unlikely to reside in host halos with $M_{\rm vir} \lesssim 1.5\times10^{12}\,M_\odot$. If we further require that $M_{\rm vir} < 3\times10^{12}\,M_\odot$, we still find that approximately 70% of hosts of LMC-like subhalos reside in hosts with $M_{\rm vir} > 2\times10^{12}\,M_\odot$.

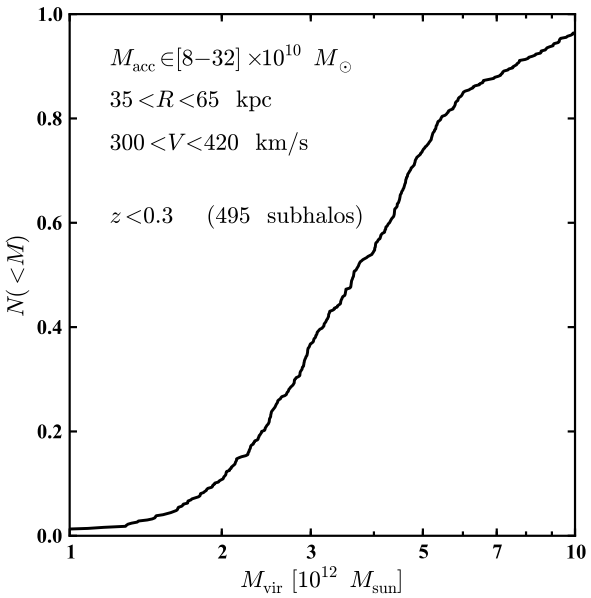

Figure 13. Distribution of halo masses in the MS-II having a satellite similar to the LMC: a mass of $8\times10^{10} < M_{\rm acc}/M_\odot < 3.2\times10^{11}\,M_\odot$, at a separation of $35 < R < 65\,$kpc from its host, and with a total velocity of $300 < V < 420\,{\rm km\,s^{-1}}$. Of all the hosts with such a subhalo at $z < 0.3$, over 90% have $M_{\rm vir} > 2\times10^{12}\,M_\odot$.

7 CONCLUSIONS

The new HST proper motions for the MCs (Kallivayalil et al. 2006a,b) have forced us to re-evaluate our understanding of their orbital history about the MW. The canonical picture, wherein the MCs are on a quasi-periodic, slowly decaying orbit around the MW, has been thrown out. We are left instead with two possibilities: (1) The MCs are on their first passage about the MW (late accretion); or (2) the MCs joined the MW > 8 Gyr ago and are now on a highly eccentric orbit, having already completed at least one passage about the MW since infall (early accretion).

In this work, we have addressed the likelihood of these two scenarios by using the MS-II to place the MCs in a cosmological context in terms of their accretion epoch, orbital properties, and masses. Our primary results can be summarized as follows:

• *LMC analogs are accreted preferentially at late times*: only 15% have $t_{\rm fc} > 7.5$ Gyr ($z_{\rm fc} > 1$), while approximately 30% have been accreted within the past 2 Gyr. Such numbers favor the late accretion scenario for the LMC.

• *The LMC's angular momentum is not anomalously high*: 30-35% of all LMC analogs have specific angular momentum matching that of the real LMC if the mass of the MW lies between $[1-3]\times10^{12}\,M_\odot$. The angular momentum of the LMC is more typical of halos at the massive end of this range than of those at the low-mass end.

• *It is exceedingly unlikely for the LMC to be on an unbound orbit*: If the mass of the MW is less than $2\times10^{12}\,M_\odot$, the LMC has an orbit that is more energetic than 90% of comparable systems (adopting the mean radial and tangential velocities of K06). 40% of MW systems with $M_{\rm vir} \in [2-3]\times10^{12}\,M_\odot$ have an LMC analog with orbital energy comparable to that of the LMC. It is highly unlikely for LMC-like subhalos to be on unbound orbits, which is the case for a low-mass MW, and none of the early-accreted LMCs are on unbound orbits. The conclusion that the LMC is in fact bound to a massive MW, and yet accreted recently, cautions against the use of backward orbital integration schemes to determine the orbital histories of satellites over cosmic time.

• *Energetically, it is difficult to accommodate a scenario where the MCs have made multiple pericentric passages*: LMCs accreted at early times are on mostly circular orbits, at odds with observations. LMCs accreted recently have not had time to complete more than one pericentric passage.

• *LMC and SMC-mass objects are not particularly uncommon in MW-mass halos*: In a refinement of the results presented in Boylan-Kolchin et al. (2010), we find that 20-32% of MW-mass halos host an LMC analog and 10-25% host an SMC analog. These results are consistent with the analysis of LMC analogs about MW type hosts located in the SDSS DR7 by Tollerud et al. (in prep.). The MCs become less typical if the host halo is lower in mass.

• *It is possible, but not probable, to find LMC-SMC binaries at z=0*: We find a small number of Milky Way-mass systems ($\sim 2.5\%$) with LMC analogs have apparent LMC-SMC binaries.

• *Subhalos with properties similar to that of the LMC reside preferentially in massive host halos*: Out of *all* dark matter halos (without restriction on mass) hosting objects with masses, velocities, and separations similar to the LMC, only 10% have $M_{\rm vir} < 2\times10^{12}\,M_\odot$, and less than 5% have $M_{\rm vir} < 1.5\times10^{12}\,M_\odot$.

Overall, our results support a scenario in which the LMC is a recent addition (in the last 4 Gyr) to a fairly massive ($M_{\rm vir} \gtrsim 1.5\times10^{12}\,M_\odot$) Milky Way.

ACKNOWLEDGMENTS

MBK thanks Simon White for many helpful discussions, including the suggestion of the "inverse" argument of §6.3, and for a careful reading of an earlier version of this manuscript. The Millennium-II Simulation databases used in this paper and the web application providing online access to them were constructed as part of the activities of the German Astrophysical Virtual Observatory. This work made extensive use of NASA's Astrophysics Data System and of the astro-ph archive at arXiv.org.

REFERENCES

Abazajian, K. N. et al. 2009, ApJS, 182, 543
Allgood, B., Flores, R. A., Primack, J. R., Kravtsov, A. V., Wechsler, R. H., Faltenbacher, A., & Bullock, J. S. 2006, MNRAS, 367, 1781
Battaglia, G. et al. 2005, MNRAS, 364, 433
Benson, A. J. 2005, MNRAS, 358, 551
Besla, G., Kallivayalil, N., Hernquist, L., Robertson, B., Cox, T. J., van der Marel, R. P., & Alcock, C. 2007, ApJ, 668, 949 [B07]
Besla, G., Kallivayalil, N., Hernquist, L., van der Marel, R. P., Cox, T. J., & Kereš, D. 2010, ApJ, 721, L97
Bett, P., Eke, V., Frenk, C. S., Jenkins, A., Helly, J., & Navarro, J. 2007, MNRAS, 376, 215
Boylan-Kolchin, M., Ma, C.-P., & Quataert, E. 2008, MNRAS, 383, 93
Boylan-Kolchin, M., Springel, V., White, S. D. M., & Jenkins, A. 2010, MNRAS, 406, 896 [BK10]
Boylan-Kolchin, M., Springel, V., White, S. D. M., Jenkins, A., & Lemson, G. 2009, MNRAS, 398, 1150 [MS-II]
Bryan, G. L., & Norman, M. L. 1998, ApJ, 495, 80
Byrd, G., Valtonen, M., McCall, M., & Innanen, K. 1994, AJ, 107, 2055
Conroy, C., Wechsler, R. H., & Kravtsov, A. V. 2006, ApJ, 647, 201
Dehnen, W., McLaughlin, D. E., & Sachania, J. 2006, MNRAS, 369, 1688
Diemand, J., Kuhlen, M., & Madau, P. 2007, ApJ, 667, 859
Eke, V. R., Cole, S., & Frenk, C. S. 1996, MNRAS, 282, 263
Fakhouri, O., & Ma, C. 2010, MNRAS, 401, 2245
Fich, M., & Tremaine, S. 1991, ARA&A, 29, 409
Freedman, W. L. et al. 2001, ApJ, 553, 47
Gardiner, L. T., & Noguchi, M. 1996, MNRAS, 278, 191
Gnedin, O. Y., Brown, W. R., Geller, M. J., & Kenyon, S. J. 2010, ApJ, 720, L108
Gottlöber, S., Klypin, A., & Kravtsov, A. V. 2001, ApJ, 546, 223
Grebel, E. K. 2005, in IAU Colloq. 198: Near-fields cosmology with dwarf elliptical galaxies, ed. H. Jerjen & B. Binggeli, 1–10
Guo, Q., White, S., Li, C., & Boylan-Kolchin, M. 2010, MNRAS, 404, 1111
James, P. A., & Ivory, C. F. 2010, arXiv:1009.2875 [astro-ph]
Jing, Y. P., & Suto, Y. 2002, ApJ, 574, 538
Kallivayalil, N., van der Marel, R. P., Alcock, C., Axelrod, T., Cook, K. H., Drake, A. J., & Geha, M. 2006a, ApJ, 638, 772 [K06]
Kallivayalil, N., van der Marel, R. P., & Alcock, C. 2006b, ApJ, 652, 1213
Khochfar, S., & Burkert, A. 2006, A&A, 445, 403
Kim, S., Staveley-Smith, L., Dopita, M. A., Freeman, K. C., Sault, R. J., Kesteven, M. J., & McConnell, D. 1998, ApJ, 503, 674
Klypin, A., Trujillo-Gomez, S., & Primack, J. 2010, arXiv:1002.3660 [astro-ph]

Komatsu, E. et al. 2009, ApJS, 180, 330
Li, Y.-S., & White, S. D. M. 2008, MNRAS, 384, 1459
Lin, D. N. C., Jones, B. F., & Klemola, A. R. 1995, ApJ, 439, 652
Majewski, S. R., Nidever, D. L., Muñoz, R. R., Patterson, R. J., Kunkel, W. E., & Carlin, J. L. 2009, in IAU Symposium, Vol. 256, IAU Symposium, ed. J. T. van Loon & J. M. Oliveira, 51–56
Maulbetsch, C., Avila-Reese, V., Colín, P., Gottlöber, S., Khalatyan, A., & Steinmetz, M. 2007, ApJ, 654, 53
Mayer, L., Mastropietro, C., Wadsley, J., Stadel, J., & Moore, B. 2006, MNRAS, 369, 1021
Moster, B. P., Somerville, R. S., Maulbetsch, C., van den Bosch, F. C., Macciò, A. V., Naab, T., & Oser, L. 2010, ApJ, 710, 903
Muñoz, R. R. et al. 2006, ApJ, 649, 201
Navarro, J. F., Frenk, C. S., & White, S. D. M. 1996, ApJ, 462, 563
—. 1997, ApJ, 490, 493 [NFW]
Piatek, S., Pryor, C., Bristow, P., Olszewski, E. W., Harris, H. C., Mateo, M., Minniti, D., & Tinney, C. G. 2007, AJ, 133, 818
Piatek, S., Pryor, C., & Olszewski, E. W. 2008, AJ, 135, 1024
Raychaudhury, S., & Lynden-Bell, D. 1989, MNRAS, 240, 195
Saha, A. et al. 2010, AJ, 140, 1719
Sakamoto, T., Chiba, M., & Beers, T. C. 2003, A&A, 397, 899
Sales, L. V., Navarro, J. F., Abadi, M. G., & Steinmetz, M. 2007, MNRAS, 379, 1475
Sawa, T., & Fujimoto, M. 2005, PASJ, 57, 429
Shattow, G., & Loeb, A. 2009, MNRAS, 392, L21
Shuter, W. L. H. 1992, ApJ, 386, 101
Springel, V. et al. 2008, MNRAS, 391, 1685
—. 2005, Nature, 435, 629
Stanimirović, S., Staveley-Smith, L., & Jones, P. A. 2004, ApJ, 604, 176
Stewart, K. R., Bullock, J. S., Wechsler, R. H., Maller, A. H., & Zentner, A. R. 2008, ApJ, 683, 597
Tormen, G. 1997, MNRAS, 290, 411
van den Bergh, S. 2006, AJ, 132, 1571
van den Bosch, F. C., Lewis, G. F., Lake, G., & Stadel, J. 1999, ApJ, 515, 50
Vieira, K. et al. 2010, AJ, 140, 1934
Vitvitska, M., Klypin, A. A., Kravtsov, A. V., Wechsler, R. H., Primack, J. R., & Bullock, J. S. 2002, ApJ, 581, 799
Wang, L., Li, C., Kauffmann, G., & De Lucia, G. 2006, MNRAS, 371, 537
Warren, M. S., Quinn, P. J., Salmon, J. K., & Zurek, W. H. 1992, ApJ, 399, 405
Watkins, L. L., Evans, N. W., & An, J. H. 2010, MNRAS, 406, 264
Weinmann, S. M., van den Bosch, F. C., Yang, X., & Mo, H. J. 2006, MNRAS, 366, 2
Wetzel, A. R. 2010, arXiv:1001.4792 [astro-ph]
Wetzel, A. R., & White, M. 2010, MNRAS, 403, 1072
Xue, X. X. et al. 2008, ApJ, 684, 1143
York, D. G. et al. 2000, AJ, 120, 1579